

# Isomorphic Ti Substitution into SBA-15 without Ti Loss and with Lower TiO<sub>2</sub> Segregation

Jae Yul Kim,<sup>†</sup> Jae Young Kim,<sup>†</sup> Hyun Joon Kang,<sup>‡</sup> Won Yong Kim,<sup>‡</sup> Young Hye Lee,<sup>‡</sup> and Jae Sung Lee<sup>\*,†</sup>

<sup>†</sup>School of Energy and Chemical Engineering, Ulsan National Institute of Science and Technology (UNIST), 50 UNIST-gil, Ulsan 689-798, Republic of Korea

<sup>‡</sup>Department of Chemical Engineering, Pohang University of Science and Technology, 77 Cheongam-ro, Pohang 790-784, Republic of Korea

## S Supporting Information

**ABSTRACT:** A convenient method has been discovered to incorporate Ti atoms isomorphically into a SBA-15 lattice without Ti loss. By hydrolysis of a Ti precursor near neutral pH instead of conventional acidic conditions, Ti loss was almost eliminated and its segregation to form TiO<sub>2</sub> particles was suppressed while the mesoporous structure remained intact.

Molecular sieve SBA-15 is mesoporous and possesses ordered hexagonal pores (space group *P6mm*) of a volume up to 1.26 cm<sup>3</sup>/g. Since its discovery in 1998 by Zhao et al.,<sup>1</sup> it has been extensively studied as a catalyst support for many reactions especially involving relatively bulky molecules.<sup>2</sup> When a part of Si is substituted isomorphically by Ti, forming an active catalytic site, the resulting Ti-SBA-15 has been widely investigated as a catalyst for epoxidation of cyclohexene<sup>3</sup> and 1-octene,<sup>4</sup> selective hydrogenation,<sup>5</sup> and photocatalytic reactions.<sup>6</sup> The results have demonstrated the possibility of replacing microporous titanium silicates like TS-1 and TS-2, or Ti/Si mixed oxides, for catalysis of bulky molecules.

The incorporation of Ti into the SBA-15 lattice is carried out in two ways: postgrafting of Ti after SBA-15 is synthesized<sup>4</sup> or incorporation in situ during the synthesis of SBA-15 by using both Ti and Si precursors in one pot of an acidic solution. The in situ method is preferred for uniform Ti distribution throughout the silica matrix of SBA-15. During the synthesis, inorganic Ti and Si precursors, titanium tetraisopropoxide (TTIP), and tetraethylorthosilicate (TEOS) interact electrostatically with an amphiphilic block copolymer named P123 (Pluronic) mediated by an acid anion. This self-assembly process can be denoted as S<sup>0</sup>–X<sup>–</sup>–I<sup>+</sup> (S<sup>0</sup> = nonionic block copolymer, X<sup>–</sup> = anion of an acidic solution like Cl<sup>–</sup>, and I<sup>+</sup> = hydrolyzed inorganic precursor, i.e., hydrolyzed TTIP and TEOS).<sup>7</sup> However, because of the high solubility of a Ti precursor in acidic media, there is significant Ti loss during the washing and filtering processes. Indeed, literature reports summarized in Table S1 in the Supporting Information (SI) indicate that 50–90% of Ti atoms initially present in the synthesis solution are lost from synthesized Ti-SBA-15 except for a single case that follows a similar conventional method. This loss makes control of the Ti content in the final product difficult and forces postsynthetic Ti analysis to be a requirement.

Another important issue in the synthesis of Ti-SBA-15 is the bonding state of Ti in SBA-15. Although many previous works in

Table S1 in the SI claimed that Ti was successfully incorporated into the SBA-15 framework, most of them did not provide unequivocal evidence supporting the claim of isomorphic Ti substitution. A most useful technique to differentiate the bonding states of Ti is X-ray absorption near-edge structure (XANES). Thus, identification of Ti atoms in a tetrahedral (*T<sub>d</sub>*) symmetry proves successful Ti incorporation into the *T<sub>d</sub>* silicate matrix of SBA-15, whereas octahedral (*O<sub>h</sub>*) symmetry indicates Ti segregation to form TiO<sub>2</sub> impurity. In our limited survey summarized in Table S1 in the SI, there is only one report that positively determined the presence of *T<sub>d</sub>* Ti in Ti-SBA-15 by the XANES study.<sup>8</sup>

In the present work, we have discovered a convenient method of pH control to incorporate Ti atoms successfully into SBA-15, keeping the mesoporous structure intact without significant Ti loss. More rewarding is the discovery that neutral pH suppresses TiO<sub>2</sub> segregation occurring in acidic conditions and produces Ti-SBA-15, where the majority of Ti atoms are incorporated isomorphically into the SBA-15 structure with *T<sub>d</sub>* symmetry. These improved properties of Ti-SBA-15 should have profound significant practical implications in catalytic and photocatalytic applications.

Tables 1 and S2 in the SI summarize the Ti/Si ratio and textural properties of Ti-SBA-15 synthesized at different pH values with a constant initial Ti/Si ratio (0.04) in the precursor solution with compositions shown in Table S3 in the SI. When Ti-SBA-15 was synthesized at the conventional acidic conditions

**Table 1. Ti/Si Ratio and Brunauer–Emmett–Teller (BET) Surface Area of a Series of Ti-SBA-15 Synthesized at Different pH Conditions**

pH	Ti/Si <sup>a</sup>	BET/(m <sup>2</sup> /g)
0.068	0.004332	754.3
4.45	0.03447	868.2
5.50	0.03882	771.7
7.00	0.03931	768.5
7.75	0.04011	836.0
8.87	0.05042	37.73

<sup>a</sup>Inductively coupled plasma atomic emission spectrometry results of Ti-SBA-15 synthesized from the precursor solution of an initial Ti/Si ratio of 0.04.

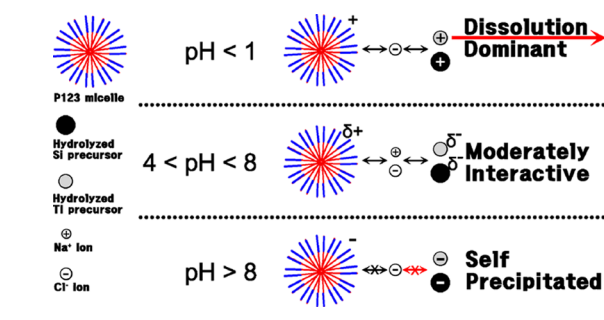
Received: March 23, 2014

Published: May 28, 2014

(pH 0.068) of the SBA-15 manufacturing process, Ti atoms as high as ~90% were lost during the filtration process following a hydrothermal step. Increasing the pH in steps to 7.75 led to a dramatic improvement in the Ti retention by almost completely eliminating the loss of Ti. At a basic pH of 8.87, dissolution of Si was noted. In addition, the pore structure of SBA-15 was destroyed as discussed later. Hence, neutral pH is the best condition to incorporate Ti atoms into a SBA-15 lattice, keeping the mesoporous structure intact and without significant Ti loss.

The marked effects of the pH on Ti loss could be understood, as depicted in Scheme 1. Under highly acidic conditions of pH

**Scheme 1. Structures of P123–Inorganic Precursor Complex Mediated by  $\text{Cl}^-$  or  $\text{Na}^+$  Ions (from HCl and NaOH Added for pH Adjustment) in the Ti Precursor Solution at Different pH Values**



<1, hydrolysis of the Ti–O–Si network is dominant.<sup>9</sup> Because the isoelectric point of  $\text{TiO}_2$  (4–4.5) is higher than that of  $\text{SiO}_2$  (2–2.5),<sup>9,10</sup> the  $\zeta$  potential of a hydrolyzed Ti precursor is more positive than that of a hydrolyzed Si precursor. Thus, Ti dissolution is much more severe in aqueous acidic conditions because of its high affinity with  $\text{H}^+$  ions. At mild acidic or neutral condition (pH 4–8), hydrolysis becomes less vigorous and the surface charges of hydrolyzed precursors for both Ti and Si are negative, so that they could be moderately associated with oxide of the poly(ethylene oxide) group in the P123 micelle mediated by a  $\text{Na}^+$  cation. Hence, preferential dissolution of Ti is suppressed. This cooperative periodic bicoordinate template, composed of hydrolyzed Si and Ti precursors, is cocondensed in a stable manner and firmly survives the distilled water filtering process. However, at the basic condition (pH > 8), both Ti and Si precursors assume the same negative charge and would self-precipitate without condensing with the P123 micelle. Hence, the templating effect of P123 is not available, and thus the hexagonal pore structure is not formed.

The global morphology of Ti-SBA-15 was examined by high-resolution transmission electron microscopy (HRTEM) for two representative samples (both with initial Ti/Si = 0.04) synthesized at acidic (pH 0.068) and neutral (pH 7.00) conditions. As shown in Figures 1 and S1 in the SI, two-dimensional (2D) hexagonal pore structures are well developed in both samples. The diameter of the hexagonal pore is about 10 nm for both cases, and mesosize channels are aligned over several hundreds of nanometers. This thin platelet with straight mesochannels densely aligned is characteristic of the SBA-15 structure. In addition, electron energy loss spectroscopy (EELS) mapping images show that Ti is uniformly distributed on this scale without apparent segregation. Thus, these HRTEM results indicate that our synthesis at neutral pH produces high-quality Ti-SBA-15 just as at acidic pH. The textural properties of Ti-

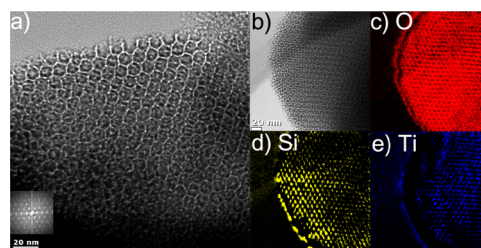


**Figure 1.** TEM images of Ti-SBA-15 synthesized at pH 7.00 pictured through the direction perpendicular to the pore axis. Selected-area electron diffraction patterns of Ti-SBA-15 are in the insets. EELS mappings are also presented (c–e).

SBA-15 synthesized at different pH values were studied in more detail in Figure S3 in the SI.

Because isomorphic substitution of Ti into a SBA-15 lattice without segregation is critical for its reactivity, XANES was employed to observe the local coordination environment of  $\text{Ti}^{IV}$ . The preedge features of Ti K-edge XANES indicate 4-, 5-, or 6-fold-coordinated Ti atoms reflecting the nature of the transition from the Ti 1s energy level to the Ti 3d/O 2p orbital. In Figure 2a, expected peaks are noted for Ti coordination with  $T_d$  or  $O_h$

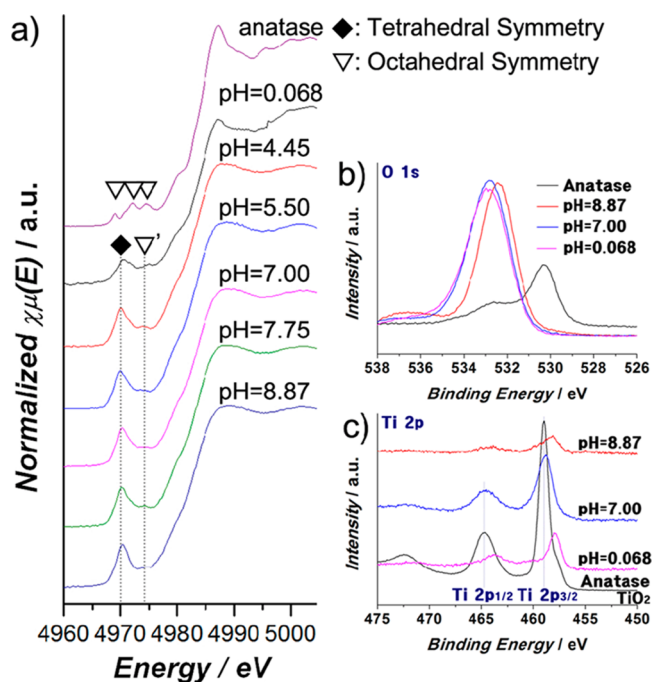


**Figure 2.** XANES (a) and XPS (b and c) of a series of Ti-SBA-15 synthesized at different pH conditions. Dotted lines in part a indicate the positions of  $T_d$  and  $O_h$  symmetry peaks. XPS of O 1s (b) and Ti 2p (c). The signal of  $\text{TiO}_2$  anatase was reduced by a factor of 20.

symmetry.<sup>2,5</sup> Because the samples were carefully dehydrated right before XANES analysis, we rule out 5-fold Ti coordination produced by surface-bound  $\text{TiOH}$  species. For Ti-SBA-15 made at pH 0.068, the spectrum is rather noisy because ~90% of Ti has been swept away from the initial composition. More importantly, the intensity of its preedge peak at 4967–4974 eV is the smallest while that at 4974 eV is the highest among the samples. The result is consistent with the presence of  $\text{TiO}_2$  with  $O_h$  symmetry, as confirmed by wide-angle X-ray diffraction (WAXD) in Figure S3d in the SI. However, other spectra of Ti-SBA-15 synthesized

at moderate pH (4–8) show the well-developed  $T_d$  symmetry peak with much lower intensity of the  $O_h$  signal.

X-ray photoelectron spectroscopy (XPS) and diffuse-reflectance (DRS) infrared Fourier transform (DRIFT; Figure S7 in the SI) studies were performed to supplement XANES results. Parts b and c of Figure 2 show a blue shift of ca. 1.5 eV in the binding energy of O 1s electrons and a red shift of ca. 0.15–0.95 eV in Ti  $2p_{3/2}$  electrons relative to those of pure  $TiO_2$  anatase. All of the results are consistent with the formation of Ti–O–Si bonds<sup>11</sup> in Ti-SBA-15. Thus, Ti has been successfully incorporated into the SBA-15 silicate framework in an atomic state, forming Ti–O–Si bonding with little segregation to form  $TiO_2$  in the Ti-SBA-15 sample of pH 7.00.

To understand the different behavior of isomorphous Ti substitution at different pH values, the hydrolysis kinetics of TTIP and TEOS were studied. At all pH values, TTIP was hydrolyzed as soon as it was dropped into the solution of P123. On the other hand, TEOS was more slowly hydrolyzed so that the rate could be studied visually at different pH values (Figure S8 in the SI) and by UV–vis DRS (Figures 3 and S9 in the SI).

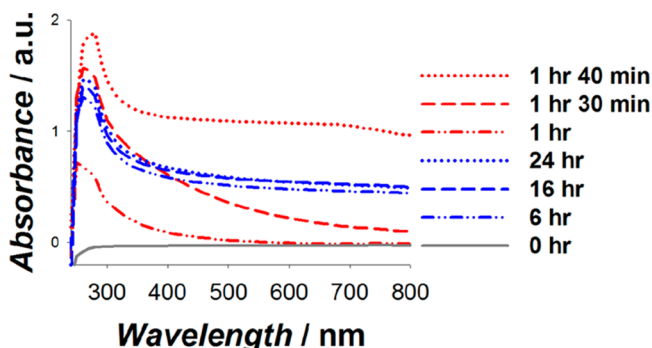


**Figure 3.** UV–vis DRS of hydrolyzed TEOS sol versus time. Red line: pH 0.068. Blue line: pH 7.00.

The intensity of the peak appearing in the range of 250–320 nm of UV–vis DRS is proportional to the concentration of the hydrolyzed TEOS.<sup>12</sup> At pH 0.068, the color of the solution changes suddenly from transparent white to a pale milky color over 10 min from 1 h 30 min to 40 min after the reaction started. The process was accompanied by a quick increase of the UV–vis signal intensity. At pH 7.00, the process proceeded slowly, and it took more than 15 h to reach the same hydrolyzed state. Hence, when Ti-SBA-15 is synthesized, the state TTIP is the same at both pH values, i.e., completely hydrolyzed, but the state of TEOS is different. At pH 0.068, hydrolysis of TEOS is rapid and completed in such a short time that hydrolyzed TEOS may not accommodate with prehydrolyzed TTIP, inducing Ti segregation. However, at pH 7.00, TEOS is hydrolyzed slowly at a constant speed enabling homogeneous mixing with prehydrolyzed TTIP. Hence, there are much less segregated phases. The presence of the brookite phase at the basic condition (pH 8.87) could be similarly understood by the higher hydrolysis rate of TEOS (Figure S9 in the SI) and higher concentration of  $OH^-$  for  $TiO_2$  aggregation.

To incorporate Ti into the SBA-15 framework to prepare Ti-SBA-15, highly acidic pH is used to accelerate slow hydrolysis of TEOS. However, 90% of Ti in the initial solution is lost under this condition. However, when the synthesis is performed under neutral pH, almost complete retention of Ti is possible. More rewarding is the discovery that neutral pH produces higher-

quality Ti-SBA-15 of a 2D hexagonal-ordered mesopore structure with less segregation of Ti atoms in the SBA-15 framework. Basic pH destroys the SBA-15 structure. Thus, the recommended pH value for synthesizing Ti-SBA-15 is near 7.00 in order to keep the structure intact, with little  $TiO_2$  segregation and without Ti loss. The procedure could also be applied to the incorporation of other elements like Al or Zr.<sup>13</sup>

## ■ ASSOCIATED CONTENT

### ■ Supporting Information

Experimental procedures, textural properties, TEM and SEM images, a  $N_2$  isotherm, SAXS, WAXD,  $t$  plots, UV–vis DRS, XANES, DRIFT, and pictures of hydrolyzed TEOS. This material is available free of charge via the Internet at <http://pubs.acs.org>.

## ■ AUTHOR INFORMATION

### Corresponding Author

\*E-mail: [jlee1234@unist.ac.kr](mailto:jlee1234@unist.ac.kr).

### Notes

The authors declare no competing financial interest.

## ■ ACKNOWLEDGMENTS

We thank Drs. S. H. Choi, T. J. Shin, and H. J. Park for X-ray absorption fine structure, small angle X-ray scattering (SAXS), and TEM measurements. This work was supported by the BK<sub>+</sub> program, Korean Centre for Artificial Photosynthesis (NRF-2011-C1AAA0001-2011-0030278), and Basic Science Research Program (2012-017247) funded by the NRF of Republic of Korea.

## ■ REFERENCES

- (1) Zhao, D.; Feng, J.; Huo, Q.; Melosh, N.; Fredrickson, G. H.; Chmelka, B. F.; Stucky, G. D. *Science* **1998**, 279, 548–552.
- (2) Sacaliuc, E.; Beale, A. M.; Weckhuysen, B. M.; Nijhuis, T. A. *J. Catal.* **2007**, 248, 235–248.
- (3) Bérubé, F.; Khadhraoui, A.; Janicke, M. T.; Kleitz, F.; Kaliaguine, S. *Ind. Eng. Chem. Res.* **2010**, 49, 6977–6985.
- (4) Melero, J. A.; Iglesias, J.; Sainz-Pardo, J.; de Frutos, P.; Blázquez, S. *Chem. Eng. J.* **2008**, 139, 631–641.
- (5) Trukhan, N. N.; Romannikov, V. N.; Shmakov, A. N.; Vanina, M. P.; Paukshtis, E. A.; Bukhtiyarov, V. I.; Kriventsov, V. V.; Danilov, I. Y.; Kholdeeva, O. A. *Microporous Mesoporous Mater.* **2003**, 59, 73–84.
- (6) Jung, W. Y.; Baek, S. H.; Yang, J. S.; Lim, K. T.; Lee, M. S.; Lee, G. D.; Park, S. S.; Hong, S. S. *Catal. Today* **2008**, 131, 437–443.
- (7) (a) Zhao, D.; Huo, Q.; Feng, J.; Chmelka, B. F.; Stucky, G. D. *J. Am. Chem. Soc.* **1998**, 120, 6024–6036. (b) Zhang, W.; Fröba, M.; Wang, J.; Tanev, P. T.; Wong, J.; Pinnavaia, T. J. *J. Am. Chem. Soc.* **1996**, 118, 9164–9171. (c) Prouzet, E.; Pinnavaia, T. J. *Angew. Chem., Int. Ed.* **1997**, 36, 516–518.
- (8) Chen, S. Y.; Tang, C. Y.; Lee, J. F.; Jang, L. Y.; Tatsumi, T.; Cheng, S. J. *Mater. Chem.* **2011**, 21, 2255–2265.
- (9) Visuvamithiran, P.; Shanthi, K.; Palanichamy, M.; Murugesan, V. *Catal. Sci. Technol.* **2013**, 3, 2340–2348.
- (10) Kim, J. Y.; Jang, J. W.; Youn, D. H.; Kim, E. S.; Choi, S. H.; Shin, T. J.; Lee, J. S. *Green Chem.* **2013**, 15, 3387–3395.
- (11) (a) Lassaletta, G.; Fernandez, A.; Espinos, J. P.; Gonzalez-Eliphe, A. R. *J. Phys. Chem.* **1995**, 99, 1484–1490. (b) Gao, X.; Bare, S. R.; Fierro, J. L. G.; Banares, M. A.; Wachs, I. E. *J. Phys. Chem. B* **1998**, 102, 5653–5666.
- (12) (a) Chang, S. Y.; Liu, L.; Asher, S. A. *J. Am. Chem. Soc.* **1994**, 116, 6739–6744. (b) Zhou, L.; Heinz, H.; Soucek, M. D.; Alemán, E. A.; Modarelli, D. A. *Silicon* **2010**, 2, 95–104.
- (13) Sun, Y.-H.; Sun, L.-B.; Li, T.-T.; Liu, X.-Q. *J. Phys. Chem. C* **2010**, 114, 18988–18995.